Catheter Visualization Using Rubber Bands and Ultrashort TE Imaging

J. Rahmer[1], and S. Krueger[1]
[1]Philips Research Europe, Hamburg, Germany

Introduction
Increasingly, interventional procedures rely on MR imaging for tracking of catheters in the body. Active catheter visualization allows highlighting the tip position in a standard MR image, but requires additional equipment and dedicated catheters [1]. In contrast, passive visualization requires only minimal device modification. Typically, susceptibility markers are attached to the device to cause local contrast in the image. However, this contrast effect is permanent and can negatively affect the anatomical information in the MR image. Moreover, it strongly depends on the imaging parameters and orientation of the markers with respect to B_0. We therefore propose to use short-T_2 material with T_2 shorter than about 1 ms as a passive marker. This material does not interfere with standard MR imaging, but can be visualized using ultrashort echo-time (UTE) sequences [2]. The short-T_2 marker can either be visualized on the background of the anatomy or it can be visualized without anatomical background using short-T_2 selective UTE imaging [3]. This work demonstrates the passive visualization of the full catheter length using 3D UTE imaging of short-T_2 rubber bands inserted into the catheter.

Methods
Figure 1(a) depicts a 3D radial UTE sequence. After a non-selective excitation pulse and a coil-dependent switching time, the free-induction decay (FID) is sampled with an optional later gradient echo [4]. Radial *k*-space profiles cover a sphere with homogeneous angular density [5]. The data is reconstructed to an isotropic 3D grid. A first echo time $TE_1 < 100$ µs enables the detection of short-T_2 materials like rubber, with T_2 below 1 ms. As a short-T_2 marker covering the complete length of a 6F catheter, two rubber filaments are inserted into one of the two lumina (Fig. 1(b)).
MR scans were performed on a clinical 1.5 T whole body scanner (Achieva 1.5T, Philips Medical Systems, Best, The Netherlands) using a single elliptical receive coil (30 x 20 cm) placed flat on the patient table. A basin was placed on the coil. Inside the basin, the catheter was mounted on plastic posts, allowing immersion of the catheter in phantom fluid. Scanning was performed using a 3D dual echo UTE sequence with a scan matrix of 128^3 and a FOV of 200 mm, yielding isotropic resolution. 32768 radial readouts were performed with TR = 4.1 ms, corresponding to an undersampling factor of 1.5 for the FID and amounting to a scan duration of 2 min 20 s. To demonstrate the short T_2 of rubber filaments, a scan of the catheter in air was performed with $TE_1/TE_2 = 0.05/1.4$ ms. Images with short-T_2 contrast were derived from dual echo scans of the catheter immersed in phantom fluid using $TE_1/TE_2 = 0.05/2.3$ ms. A 3D difference data set was generated by subtraction of the 2nd echo from the 1st (FID).

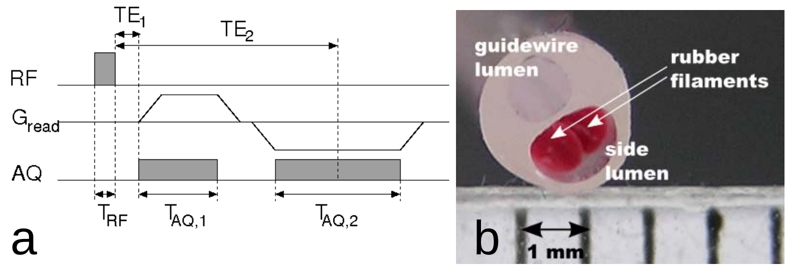

Figure 1: 3D UTE sequence and catheter with short-T2 marker. (a) A non-selective excitation pulse is applied before 3D radial dual echo (FID/echo) sampling. (b) Rubber filaments are placed into the side lumen of a 6F catheter.

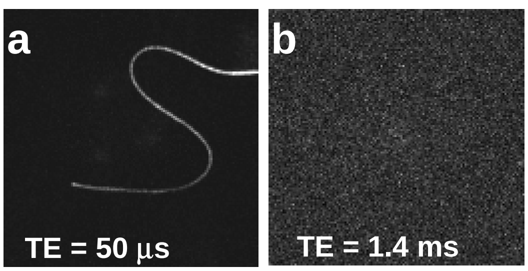

Figure 2: MIP of 3D UTE dual echo data of the catheter in air. At ultrashort TE = 50 µs, the rubber filaments yield signal, which is already decayed at TE larger than 1 ms.

Results and Discussion
Figure 2 shows a maximum intensity projection (MIP) of the dual echo data sets, demonstrating the high signal obtained from the rubber filaments at ultrashort TE = 50 µs (a). At TE = 1.4 ms, the rubber signal is already decayed due to its sub-millisecond T_2 (b). Figures 3(a-c) show a coronal slice through the phantom-filled basin. At ultrashort TE (a), both phantom fluid and rubber yield bright signal, whereas the rubber appears black at the later echo time (b). The plastic mounting of the catheter appears as black discs and boxes in the images. A difference image between FID and echo highlights short-T_2 components only (c), so that the rubber filaments appear bright (arrow). Slight edge artifacts around the plastic parts are visible as well. Figure 3(d) shows a MIP through the difference data set, visualizing the complete length of the catheter. At this stage, 3D scan times are too long for real-time catheter tracking. However, by putting more rubber into the catheter, by choosing short-T_2 material with higher proton content, or by even fabricating the catheter itself from appropriate short-T_2 material, the marker signal could be substantially increased. This would allow using strong radial undersampling as applied in angiography to push acquisition time per frames down to a few seconds [6]. Alternatively, 2D UTE scanning could be used to arrive at shorter scan times for real time tracking. On the other hand, the 3D technique can also be used in combination with other device tracking methods and offers the possibility to acquire a complete 3D image as a fallback or for the detection of possible loop formation in the catheter.

Conclusion
Short-T_2 material can be used to selectively visualize the complete length of a catheter for MR catheter tracking in 3D, without the need for additional hardware. A short-T_2 selective UTE exam is used for visualization. The technique requires only minor device modifications and is thus also suited as an add-on to existing device visualization methods. Larger devices or application of material with higher proton content may allow higher temporal resolution for quasi real-time tracking in the future.

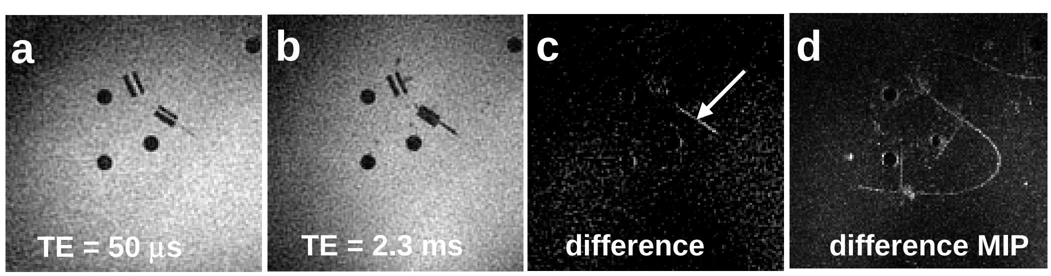

Figure 3: Single slice and MIP from 3D UTE data of the catheter in phantom fluid. The UTE image shows high signal from phantom fluid and catheter, while the catheter is black at TE = 2.3 ms. The difference image highlights the catheter only (arrow). A MIP of the 3D difference image reveals the full length of the catheter. Discs and boxes in the images correspond to plastic parts used for mounting the catheter.

References
[1] Weiss S *et al*. Magn Reson Med 2004;52:860-8. [2] Robson MD *et al*. J Comput Assist Tomogr 2003;27:825-46. [3] Rahmer J *et al*. Magn Reson Mater Phy 2007;20:83-92. [4] Glover GH *et al.*, J. Magn. Reson. Imaging **2**, 47-52 (1992). [5] Wong S *et al.*, Magn. Reson. Med. 1994;32:778-84. [6] Barger AV *et al.*, Magn. Reson. Med. 2002;48:297-305.